ANOMALY SUBSPACE DETECTION BASED ON A MULTI-SCALE MARKOV RANDOM FIELD MODEL

Arnon Goldman and Israel Cohen

Department of Electrical Engineering, Technion - Israel Institute of Technology
Technion City, Haifa 32000, Israel
goldman@tx.technion.ac.il, icohen@ee.technion.ac.il

ABSTRACT

In this paper, we introduce a multi-scale Gaussian Markov random field (GMRF) model and a corresponding anomaly subspace detection algorithm. The proposed model is based on a multi-scale wavelet representation of the image, independent components analysis (ICA), and modeling each independent component as a GMRF. The anomaly detection is subsequently carried out by applying matched subspace detector (MSD) to the innovations process of the GMRFs, incorporating a priori information about the targets. The robustness of the proposed approach is demonstrated with application to automatic detection of airplanes on synthetic cloudy sky backgrounds.

1. INTRODUCTION

Gaussian Markov random field (GMRF) modeling has been applied extensively for segmentation and synthesis of texture images [1], [2], [3], [4]. G. G. Hazel has developed in [5] an anomaly detection technique, based on the GMRF model. The detection is carried out with no assumptions about the nature of the targets, other than that they are rare. A single hypothesis scheme is used for the detection of regions in a given image, which appear unlikely with respect to the probabilistic model of the image. When a typical signature of the target is available, the detection can be carried out by using the matched signal detector. In many applications, the matched signal detector is replaced by a matched subspace detector (MSD) - a generalization of the matched filter, as presented in [6]. The MSD considers the problem of detecting subspace signals in subspace interference and additive noise.

In natural clutter images, scene elements often appear to have several periodical patterns, of various period lengths. In this case, the GMRF model may not sufficiently describe the clutter image. Deviations of the clutter image from the GMRF model influence the detection performance by increasing the false alarm rate. The detection performance is also influenced by the use of *a priori* information about the targets. Anomaly detection is carried out with no assumptions about the nature of the targets. In real detection problems, some a priori information about the targets is often available. Using this information for rejecting anomalies which do not resemble targets, may improve the detection performance.

In this paper, we introduce a multi-scale GMRF model and a corresponding anomaly subspace detection algorithm. The proposed model is based on a multi-scale wavelet representation of the image and independent component analysis (ICA). We generate from a given image, three-dimensional data and each layer in the data is then modeled as a GMRF with a different set of parameters. The detection is subsequently carried out by applying MSD to the innovation process (prediction error) of the GMRF of each layer in the data. The MSD incorporates the a priori information about the targets into the detection process and thus improves the detection performance.

The structure of the paper is as follows: In Section 2, we introduce the multi-scale GMRF. In Section 3, we develop the anomaly subspace detection algorithm. In Section 4, we demonstrate the application of the proposed algorithm to automatic target detection, and compare the results to those obtained by a competing method.

2. THE MULTI-SCALE GMRF MODEL

Let $Y(\mathbf{s})$ denote an image, and let $\mathcal{G} = \{G_1, G_2, ..., G_n\}$ denote a given set of multi-scale spatially invariant filters (*e.g.* scaling and wavelet filters). We generate from the image a multi-scale image, $\mathbf{Y}$, by applying the filters to the image Y and concatenating the results in the third dimension:

$$Y_i = Y * G_i \ , \ i = 1, ..., n \tag{1}$$

$$\mathbf{Y}(\mathbf{s}) = [Y_1(\mathbf{s}), Y_2(\mathbf{s}), ..., Y_n(\mathbf{s})] \tag{2}$$

where $*$ denotes 2-dimensional convolution. The result $\mathbf{Y}$ is a 3-dimensional representation of the image, thus each pixel is now transformed to a vector. The Karhunen-Loéve transform (KLT) can be applied to $\mathbf{Y}(\mathbf{s})$, for generating a multi-scale image, $\mathbf{T}(\mathbf{s})$, with independent layers. $\mathbf{T}(\mathbf{s})$ has p layers representing the top p independent components of $\mathbf{Y}(\mathbf{s})$. Let K denote a matrix whose columns are the top p eigen vectors of the covariance matrix of $\mathbf{Y}(\mathbf{s})$. $\mathbf{T}(\mathbf{s})$ is then given by:

$$\mathbf{T}(\mathbf{s}) = K^{\mathrm{T}}\mathbf{Y}(\mathbf{s}). \tag{3}$$

We assume that there is a set of filters, $\mathcal{G}$, such that each image layer, $\mathbf{T}_\ell(\mathbf{s})$, can be modeled as a GMRF with a different set of parameters. We denote the weight coefficient estimated for neighbor $\mathbf{r} \in \mathcal{R}$, and for the ℓ-th layer of $\mathbf{T}(\mathbf{s})$ by $\theta_\ell(\mathbf{r})$, and the innovations process of the ℓ-th layer by $\varepsilon_\ell(\mathbf{s})$. As a GMRF, $\mathbf{T}_\ell(\mathbf{s})$ is given by:

$$\mathbf{T}_\ell(\mathbf{s}) = \sum_{\mathbf{r}\in\mathcal{R}} \theta_\ell(\mathbf{r})\mathbf{T}(\mathbf{s}+\mathbf{r}) + \varepsilon_\ell(\mathbf{s}). \tag{4}$$

Let $\rho_\ell^2 = E\{\varepsilon_\ell^2(\mathbf{s})\}$ denote the variance of the innovations of the ℓ-th layer. Woods [2] showed that the innovations process of a GMRF is spatially correlated with covariance given by:

$$E\{\varepsilon_\ell(\mathbf{s})\,\varepsilon_\ell(\mathbf{s}+\mathbf{r})\} = \begin{cases} \rho_\ell^2, & \text{if } \mathbf{r} = (0,0) \\ -\theta_\ell(\mathbf{r})\rho_\ell^2, & \text{if } \mathbf{r} \in N \\ 0, & \text{otherwise.} \end{cases} \tag{5}$$

$\mathbf{T}(\mathbf{s})$ is then given by the following equation:

$$\mathbf{T}(\mathbf{s}) = \sum_{\mathbf{r}\in\mathcal{R}} \Theta_{\mathbf{r}}\mathbf{T}\left(\mathbf{s}+\mathbf{r}\right) + \varepsilon\left(\mathbf{s}\right) \tag{6}$$

where Θ_r is the following diagonal matrix:

$$\Theta_r = \text{diag}(\theta_1\left(\mathbf{r}\right), \theta_2\left(\mathbf{r}\right), ..., \theta_p\left(\mathbf{r}\right)) \tag{7}$$

and $\boldsymbol{\varepsilon}\left(\mathbf{s}\right)$ is a vector of the innovations in pixel $\mathbf{s}$ in the different layers of $\mathbf{T}\left(\mathbf{s}\right)$:

$$\boldsymbol{\varepsilon}\left(\mathbf{s}\right) = \left[\varepsilon_1\left(\mathbf{s}\right), \varepsilon_2\left(\mathbf{s}\right), ..., \varepsilon_p\left(\mathbf{s}\right)\right]^{\mathrm{T}}. \tag{8}$$

Various methods for GMRF model estimation were developed over the years, *e.g.*, [5], [1], [7], [8], [9]. A computationally efficient method for the GMRF model estimation is the least squares method, described in details in Hazel [5]. The multi-scale GMRF model estimation is based on the estimation of the GMRF parameters for each layer of $\mathbf{T}(\mathbf{s})$, using the least squares method. The estimate of Θ_r can be directly obtained from the least squares estimates of $\theta_\ell\left(\mathbf{r}\right)$ for $\mathbf{r}\in\mathcal{R}$ and $\ell = 1\ldots p$. Subsequently, we can estimate the innovations process (prediction error), $\widehat{\boldsymbol{\varepsilon}}\left(\mathbf{s}\right)$, by:

$$\widehat{\boldsymbol{\varepsilon}}\left(\mathbf{s}\right) = \mathbf{T}(\mathbf{s}) - \sum_{\mathbf{r}\in\mathcal{R}} \widehat{\Theta_r}\mathbf{T}\left(\mathbf{s}+\mathbf{r}\right). \tag{9}$$

3. ANOMALY DETECTION

In this section, we introduce an anomaly subspace detection method based on a MSD and the multi-scale GMRF model introduced in the previous section.

Scharf and Friedlander [6] formulated a MSD for the general problem of detecting subspace signals in subspace interference and additive white Gaussian noise. Here, the anomaly detection is based on a statistical model which better describes the background clutter and the noise. We formulate a modified MSD for detection of subspace signals in subspace interference and additive noise which follows the multi-scale GMRF model, proposed in the previous section.

Let $\{\mathbf{h}_j | j = 1,\ldots,u\}$ and $\{\mathbf{s}_k | k = 1,\ldots,v\}$ denote two sets of image chips, which span the signal and interference subspaces of image Y, respectively. The image chips are all of the same size:$N_x \times N_y$ pixels, which is usually much larger than the size of the neighborhood $\mathcal{R}$. It should be large enough for containing shapes which span the signal and interference subspaces.

We assume that image Y contain mainly noise, which follows the multi-scale GMRF model, and that the target and interference signals are rare. Let $\mathcal{D}_p$ denote an operator which calculates the prediction error, $\widehat{\boldsymbol{\varepsilon}}(\mathbf{s})$, of the multi-scale GMRF model with p independent components. $\mathcal{D}_p$ is defined by using (1), (3), and (9), as follows:

$$\begin{aligned}\widehat{\boldsymbol{\varepsilon}}(\mathbf{s}) &= \left[\widehat{\varepsilon}_1\left(\mathbf{s}\right), \widehat{\varepsilon}_2\left(\mathbf{s}\right), ..., \widehat{\varepsilon}_p\left(\mathbf{s}\right)\right]^{\mathrm{T}} = \mathcal{D}_p Y(\mathbf{s}) = \\ &= K^{\mathrm{T}}\mathbf{Y}(\mathbf{s}) - \sum_{\mathbf{r}\in\mathcal{R}} \boldsymbol{\Theta}_{\boldsymbol{r}} K^{\mathrm{T}}\mathbf{Y}(\mathbf{s}+\mathbf{r}).\end{aligned} \tag{10}$$

Let $\mathbf{n}_\ell(\mathbf{s})$ denote the column stack ordering of an $N_x \times N_y$ pixels image-chip of $\widehat{\varepsilon}_\ell$ around $\mathbf{s}$:

$$\mathbf{n}_\ell(\mathbf{s}) = \text{vec}(\{\widehat{\varepsilon}_\ell(\mathbf{t}) | \mathbf{t} \in [N_x \times N_y \text{ image chip around } \mathbf{s}]\}). \tag{11}$$

We define H_ℓ and S_ℓ as follows:

$$\begin{aligned} H_\ell &= \left[\text{vec}\left([\mathcal{D}_p\mathbf{h}_1]_\ell\right)\ \text{vec}\left([\mathcal{D}_p\mathbf{h}_2]_\ell\right)\ ...\ \text{vec}\left([\mathcal{D}_p\mathbf{h}_u]_\ell\right)\right] \\ S_\ell &= \left[\text{vec}\left([\mathcal{D}_p\mathbf{s}_1]_\ell\right)\ \text{vec}\left([\mathcal{D}_p\mathbf{s}_2]_\ell\right)\ ...\ \text{vec}\left([\mathcal{D}_p\mathbf{s}_v]_\ell\right)\right]\end{aligned} \tag{12}$$

where $[\cdot]_\ell$ denotes the ℓ-th layer of the 3-dimensional data.

Let $\langle H_\ell\rangle$ denote the signal subspace, spanned by the columns of matrix H_ℓ and let $\langle S_\ell\rangle$ denote the interference subspace, spanned by the columns of matrix S_ℓ. We denote the additive noise by $\mathbf{b}_\ell$. The problem is to determine whether the sample vector $\mathbf{n}_\ell$ contains a target signal. The target signal $\mathbf{x}_\ell$ can be described as a linear combination of the columns of H_ℓ *i.e.*, $\mathbf{x}_\ell = H_\ell\boldsymbol{\psi}_\ell$, where $\boldsymbol{\psi}_\ell$ is a vector of coefficients. The interference signal is described similarly, using the matrix S_ℓ and the coefficients vector $\boldsymbol{\phi}_\ell$. Considering the detection problem, we define two hypotheses, H_0 and H_1 which indicate, respectively, absence and presence of target signal in the vector $\mathbf{n}_\ell$:

$$\begin{aligned} H_0 &: \mathbf{n}_\ell = S_\ell\boldsymbol{\phi}_\ell + \mathbf{b}_\ell \\ H_1 &: \mathbf{n}_\ell = H_\ell\boldsymbol{\psi}_\ell + S_\ell\boldsymbol{\phi}_\ell + \mathbf{b}_\ell. \end{aligned} \tag{13}$$

Let P_{S_ℓ} denote the projection of a vector onto the subspace $\langle S_\ell\rangle$:

$$P_{S_\ell}\mathbf{n}_\ell(\mathbf{s}) = S_\ell({S_\ell}^{\mathrm{T}}S_\ell)^{-1}{S_\ell}^{\mathrm{T}}\mathbf{n}_\ell(\mathbf{s}) \tag{14}$$

and let $P_{H_\ell S_\ell}$ denote the projection of a vector onto the subspace $\langle H_\ell S_\ell\rangle$, spanned by the columns of the concatenated matrix $\begin{bmatrix} H_\ell & S_\ell \end{bmatrix}$. The maximum likelihood estimates of the additive noise vector, $\mathbf{b}_\ell$, under H_0 and under H_1 are denoted by $\widehat{\mathbf{b}}^\ell_{H_0}$ and $\widehat{\mathbf{b}}^\ell_{H_1}$, respectively. These estimates are obtained by subtracting from $\mathbf{n}_\ell$ the components which lie in the signal and interference subspaces as follows:

$$\begin{aligned} \widehat{\mathbf{b}}^\ell_{H_0} &= (I - P_{S_\ell})\mathbf{n}_\ell \\ \widehat{\mathbf{b}}^\ell_{H_1} &= (I - P_{H_\ell S_\ell})\mathbf{n}_\ell \end{aligned} \tag{15}$$

$\mathbf{b}_\ell$ is the innovations process of a GMRF and therefore is normally distributed with zero mean. We denote the covariance matrix of $\mathbf{b}_\ell$ by $\rho^2_\ell\Phi_\ell$, where ρ^2_ℓ is the variance of $\mathbf{b}_\ell$. $\rho^2_\ell\Phi_\ell$ is obtained by using (5).

The detection problem can be formulated as a generalized likelihood ratio test (GLRT) between H_0 and H_1. The log-likelihood ratio, L_ℓ, calculated based on the ℓ-th layer of the innovations process is given by:

$$\begin{aligned} L_\ell(\mathbf{s}) &= 2ln\left[\frac{Pr(\mathbf{b}_\ell(\mathbf{s})|H_0)}{Pr(\mathbf{b}_\ell(\mathbf{s})|H_1)}\right] = \\ &= 2ln\left[\frac{\exp\left(\frac{\left[\Phi_\ell^{-1/2}\widehat{\mathbf{b}}^\ell_{H_0}(\mathbf{s})\right]^2}{2\rho^2_\ell}\right)}{\exp\left(\frac{\left[\Phi_\ell^{-1/2}\widehat{\mathbf{b}}^\ell_{H_1}(\mathbf{s})\right]^2}{2\rho^2_\ell}\right)}\right] = \\ &= \frac{1}{\rho^2_\ell}\left[\left\|\Phi_\ell^{-1/2}\widehat{\mathbf{b}}^\ell_{H_0}(\mathbf{s})\right\|_2^2 - \left\|\Phi_\ell^{-1/2}\widehat{\mathbf{b}}^\ell_{H_1}(\mathbf{s})\right\|_2^2\right]. \end{aligned} \tag{16}$$

The log-likelihood ratio, based on p layers of the innovations process is given by $L(\mathbf{s}) = \sum_{\ell=1}^{p} L_\ell(\mathbf{s})$ as follows:

$$\begin{aligned} L \quad (\mathbf{s}) = \\ = \quad \sum_{\ell=1}^{p} \frac{1}{\rho_\ell^2} \left[\left\| \Phi_\ell^{-1/2} \widehat{\mathbf{b}}_{H_0}^{\ell}(\mathbf{s}) \right\|_2^2 - \left\| \Phi_\ell^{-1/2} \widehat{\mathbf{b}}_{H_1}^{\ell}(\mathbf{s}) \right\|_2^2 \right] = \\ = \quad \sum_{\ell=1}^{p} \frac{1}{\rho_\ell^2} [\Phi_\ell^{-1/2} \mathbf{n}_\ell(\mathbf{s})]^{\mathrm{T}} \left(P_{H_\ell S_\ell} - P_{S_\ell} \right) [\Phi_\ell^{-1/2} \mathbf{n}_\ell(\mathbf{s})]. \end{aligned} \tag{17}$$

The signal-to-noise ratio (SNR) is the ratio between the signal and the noise in terms of intensity. We define the SNR as the second power of the ratio between the signal, which do not lie in the interference subspace, and the standard deviation of the noise, as follows:

$$SNR = \sum_{l=1}^{p} \frac{1}{\rho_\ell^2} \mathbf{x}_\ell{}^{\mathrm{T}} [I - P_{\widetilde{S}_\ell}] \mathbf{x}_\ell. \tag{18}$$

Let u denote the rank of the signal subspace and let $q = up$. L is a sum of squared independent normally distributed variables and therefore is chi-square distributed with q degrees of freedom, as follows:

$$L \sim \begin{cases} \chi_q^2(0) & \text{, under } H_0 \\ \chi_q^2(SNR) & \text{, under } H_1. \end{cases} \tag{19}$$

Under hypothesis H_1, the non-centrality parameter of the chi-square distribution of L is equal to the SNR [6]. The decision rule is based on thresholding the log-likelihood ratio using the threshold η as follows:

$$\xi = \begin{cases} H_0 & \text{if} \quad L \leq \eta \\ H_1 & \text{if} \quad L > \eta. \end{cases} \tag{20}$$

Given (19) and (20), the probabilities of false-alarm and detection are:

$$P_{FA} = 1 - P\left[\chi_q^2(0) \leq \eta\right] \tag{21}$$

$$P_D = 1 - P\left[\chi_q^2(SNR) \leq \eta\right]. \tag{22}$$

Figure 1 presents a flow chart with the main steps of the algorithm:

1. **Generation of a Multi-Scale Representation:** The image Y is filtered by a set of spatial filters, $\mathcal{G}$, using (1), in order to create its multi-scale representation, $\mathbf{Y}$.
2. **Independent Components Analysis:** The KLT is applied to the vectors of the multi-scale representation, $\mathbf{Y}$, using (3). The result is a multi-scale representation, $\mathbf{T}$, with independent layers.
3. **Estimation of the Innovations Process:** The GMRF parameters set is separately estimated for each layer of $\mathbf{T}$. The sample innovations, $\widehat{\varepsilon}_\ell(\mathbf{s})$, are calculated for each layer, ℓ, of $\mathbf{T}$ using (10) and the estimated parameters.
4. **Matched Subspace Detector:** S_ℓ and H_ℓ are calculated using (12). A MSD is formed and the log-likelihood ratio, L, is calculated for each pixel using (17).
5. **Decision Rule (Thresholding):** The decision rule given in (20) is applied to the log-likelihood ratio, L, in order to determine whether a pixel $\mathbf{s}$ belongs to a target. The threshold, η, is determined by the admissible false alarm rate (FAR) using (21).

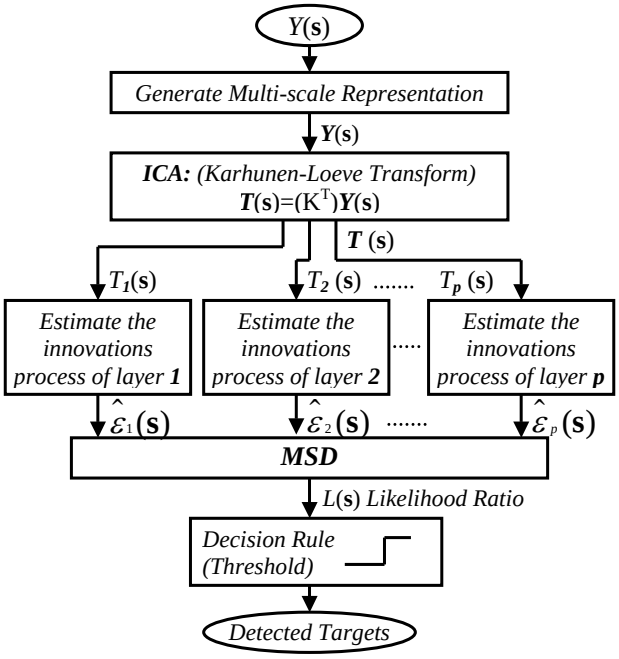

Fig. 1. Flow chart of the proposed algorithm implementation.

4. EXPERIMENTAL RESULTS

In this section, we present the results of applying the proposed model and algorithm to synthetic images of airplanes on cloudy background. The example demonstrate the robustness and flexibility of the algorithm.

Kashyap and Chellappa [1] proposed a method for synthetic generation of images which follow the GMRF model. The method is based on an expression of the GMRF model in terms of white noise. The synthetic cloudy background is generated based on this method:

1. Three random images are generated based on the GMRF model, using three different sets of parameters.
2. A weighted sum of the three images is calculated. The result contains several periodical patterns with different period lengths.
3. A small airplane image is planted in the center of the background image.

Figure 2 shows examples of target detection in synthetic images using the proposed anomaly detection algorithm. Figure 2(a) presents two images of airplanes on synthetic cloudy sky background. A multi-scale representation of each image is obtained by applying undecimated wavelet transform with 2 scale levels to the image. Accordingly, the layers of the multi-scale representation are the result of convolving the image with the wavelet basis images. We employ a signal subspace that is constructed from the span of 4 image chips of 11×11 pixels. The image chips contain bar shapes in different orientations: 0°, 45°, 90°, and 135° which resemble the fuselage of airplane targets. Figure 2(b) shows the likelihood ratios (degree of anomality) calculated using (16) for the images in Fig. 2(a). The targets, marked by circles, are detected by thresholding the likelihood ratio. The threshold is determined

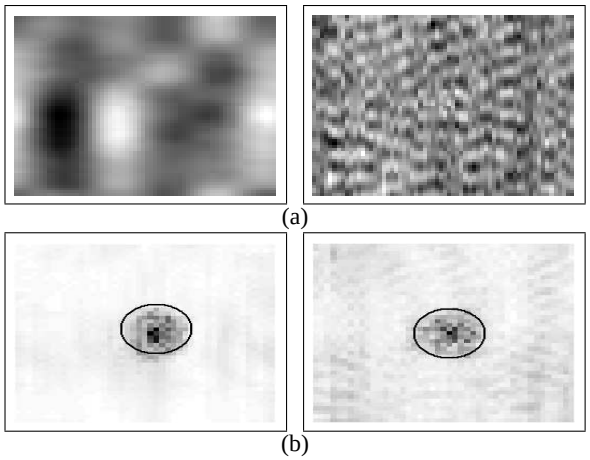

Fig. 2. (a) Synthetic images of airplanes on cloudy sky backgrounds ; (b) likelihood ratios obtained by the proposed anomaly detection algorithm. The detected targets are marked by circles.

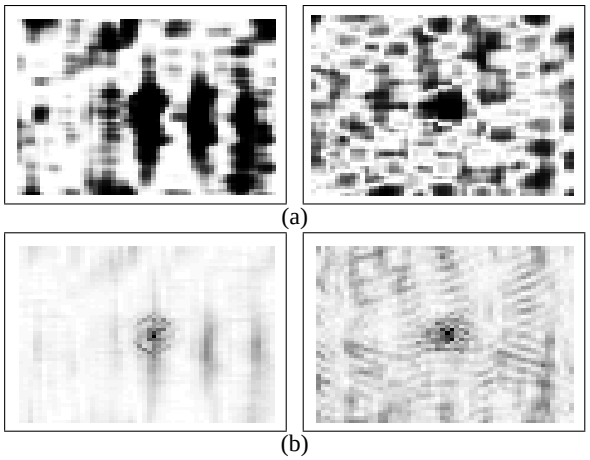

Fig. 3. A comparison between detection methods, applied to the images in Fig. 2(a). (a) Result of *Method I* ; (b) Result of *Method II*. The images in (a) seem to have higher false alarm rate (FAR) than those in (b).

by the admissible level of the FAR. The example demonstrates the robustness of the algorithm in presence of different patterns of background. The image chips which span the signal subspace (target subspace) are simple and generally do not require detailed information about the targets.

In order to demonstrate the performance of the proposed algorithm, we compared its results with those of competing methods, by applying them to the same synthetic images. The competing methods examined in this section employ a conventional GMRF model. Furthermore, the target detection is carried out as follows:

Method I: A single hypothesis scheme is applied to the estimated innovations process for the detection of regions in the image, which appear unlikely with respect to its normal distribution [5].

Method II: A MSD is applied to the estimated innovations process.

Figure 3(a) presents the results of *Method I*, applied to the synthetic images in Fig. 2(a). The results are noisy and the targets can not be distinguished from the background. Figure 3(b) shows the results of *Method II* applied to the synthetic images in Fig. 2(a). The likelihood ratios reveal the targets, which are almost unnoticeable by a human viewer due to their weak signatures. The results obtained by *Method II* seem to be noisier compared to the results of the proposed method. Using (18), we calculated the SNRs obtained by *Method II* and the proposed method for the images in Fig. 2(a). The results show significant improvement: the SNRs obtained for the left image and the right image by *Method II* are 30dB and 21dB respectively, while the SNRs obtained by the proposed method are 33dB and 27dB.

5. CONCLUSION

We have introduced a multi-scale GMRF model and a corresponding anomaly subspace detection algorithm. The proposed model is based on a multi-scale representation of the image and ICA. The detection is carried out by applying MSD to the innovations process of the estimated multi-scale GMRF. The MSD incorporates the available *a priori* information about the targets into the detection process and thus improves the detection performance compared to single hypothesis tests. The experimental results demonstrated the advantage of the proposed method over competing methods.

6. REFERENCES

[1] R. L. Kashyap and R. Chellappa, "Estimation and choice of neighbors in spatial-interaction models of images," *IEEE Transactions on Information Theory*, vol. IT-29, no. 1, pp. 60–72, January 1983.

[2] J. W. Woods, "Two-dimensional discrete Markovian fields," *IEEE Transactions on Information Theory*, vol. IT-18, no. 2, pp. 101–109, March 1972.

[3] X. Descombes and M. Sigelle and F. Preteux, "Estimating gaussian Markov random field parameters in a nonstationary framework: Application to remote sensing imaging," *IEEE Transactions on Image Processing*, vol. 8, no. 4, pp. 490–502, April 1999.

[4] R. Paget and I. D. Longstaff, "Texture synthesis via noncausal nonparametric multiscal Markov random field," *IEEE Transactions on Image Processing*, vol. 7, no. 6, pp. 925–931, June 1998.

[5] G. G. Hazel, "Multivariate gaussian GMRF for multispectral scene segmantation and anomaly detection," *IEEE Transactions on Geoscience and Remote Sensing*, vol. 38, no. 3, pp. 1199–1211, May 2000.

[6] L. L. Scharf and B. Friedlander, "Matched subspace detectors," *IEEE Transactions on Signal Processing*, vol. 42, no. 8, pp. 2146–2156, August 1994.

[7] S. M. Schweizer and J. M. F. Moura, "Efficient detection in hyperspectral imagery," *IEEE Transactions on Image Processing*, vol. 10, no. 4, pp. 584–597, April 2001.

[8] S. M. Schweizer and J. M. F. Moura, "Hyperspectral imagery: Clutter adaption in anomaly detection," *IEEE Transactions on Information Theory*, vol. 46, no. 5, pp. 1855–1871, August 2000.

[9] P. Zhao and J. Litva, "Consistency of modified LS estimation method for identifying 2-D noncausal SAR model parameters," *IEEE Transactions on Automatic Control*, vol. 40, no. 2, pp. 316–320, February 1995.